Dipeptidomimetic Ketomethylene Isosteres as Pro-moieties for Drug Transport via the Human Intestinal Di-/Tripeptide Transporter hPEPT1: Design, Synthesis, Stability, and Biological Investigations

Jon Våbenø,[†] Carsten Uhd Nielsen,[‡] Truls Ingebrigtsen,[†,⊥] Tore Lejon,[⊥] Bente Steffansen,[‡] and Kristina Luthman*[,†,§]

Department of Medicinal Chemistry, Institute of Pharmacy, University of Tromsø, N-9037 Tromsø, Norway; Department of Pharmaceutics, The Danish University of Pharmaceutical Sciences, Universitetsparken 2, DK-2100 Copenhagen, Denmark; Department of Chemistry, University of Tromsø, N-9037 Tromsø, Norway; and Department of Chemistry, Medicinal Chemistry, Göteborg University, SE-412 96 Göteborg, Sweden

Received January 26, 2004

Five dipeptidomimetic-based model prodrugs containing ketomethylene amide bond replacements were synthesized from readily available α,β-unsaturated γ-ketoesters. The model drug (BnOH) was attached to the C-terminus or to one of the side chain positions of the dipeptidomimetic. The stability, the affinity for the di-/tripeptide transporter hPEPT1, and the transepithelial transport properties of the model prodrugs were investigated. ValΨ[$COCH_2$]-Asp(OBn) was the compound with highest chemical stability in buffers at pH 6.0 and 7.4, with half-lives of 190 and 43 h, respectively. All five compounds showed high affinity for hPEPT1 (K_i values < 1 mM), and PheΨ[$COCH_2$]Asp(OBn) and ValΨ[$COCH_2$]Asp(OBn) had the highest affinities with K_i values of 68 and 19 μM, respectively. An hPEPT1-mediated transport component was demonstrated for the transepithelial transport of three compounds, a finding that was corroborated by hPEPT1-mediated intracellular uptake. The results indicate that the stabilized Phe-Asp and Val-Asp derivatives are promising pro-moieties in a prodrug approach targeting hPEPT1.

Introduction

In recent years the human di/tri-peptide transporter hPEPT1[1,2] has been extensively studied[3] due to its ability to not only transport di- and tripeptides but also peptidomimetic drugs, e.g. β-lactam antibiotics[4] and angiotensin converting enzyme (ACE) inhibitors,[5] across the intestinal epithelium. Additionally, a number of prodrugs based on amino acid or dipeptide pro-moieties have been shown to be substrates for hPEPT1, including valacyclovir (the L-valyl ester of acyclovir),[6] Gly-Val-acyclovir,[7] and the stabilized model prodrug D-Asp-(OBn)-Ala.[8] Thus, a drug/prodrug delivery approach targeting hPEPT1 is promising, and an extensive search for suitable pro-moieties has been initiated.[9−11]

hPEPT1 has been termed a low affinity/high capacity transporter[12] since di- and tripeptides, its natural substrates, typically have K_i values in a narrow range of 0.1−3.0 mM.[13] We have earlier published hPEPT1 affinity and transport data on a series of five Phe-Gly dipeptidomimetics which showed that the ketomethylene isostere had a K_i value for hPEPT1 of 0.40 mM (in this context considered as high affinity) and was transported into and across Caco-2 cells in an hPEPT1-dependent manner.[14] These results encouraged us to further investigate the use of pro-moieties containing the ketomethylene isostere. Hence, the five model prodrugs **1**−**5** (Figure 1) were synthesized. The compounds are derivatives of PheΨ[$COCH_2$]Gly (**1**), ValΨ-[$COCH_2$]Gly (**2**), PheΨ[$COCH_2$]Asp (**3**), ValΨ[$COCH_2$]-Asp (**4**) and AspΨ[$COCH_2$]Gly (**5**), to which the model drug benzyl alcohol (BnOH) was linked via an ester bond to either the C-terminus or to carboxylic acid groups in the amino acid side chain positions. In the present study we report the design and synthesis, and studies of the chemical and biological stabilities (buffer stability in the absence and presence of Caco-2 cells, respectively), the affinities for hPEPT1 and the transport properties, of these dipeptidomimetic model prodrugs.

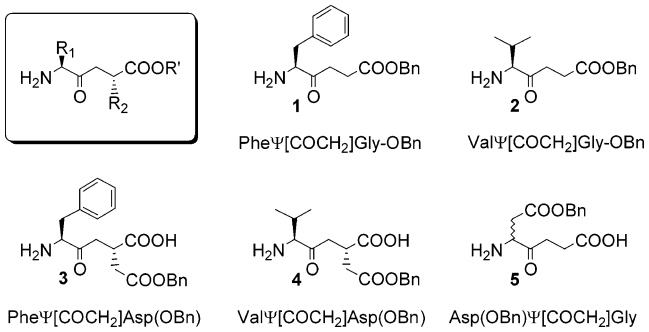

Figure 1. Structures of the synthesized dipeptidomimetic model prodrugs.

Design. Our previous study on Phe-Gly dipeptidomimetics showed that the Phe-Gly ketomethylene isostere **26** had affinities for hPEPT1 and rPEPT2 similar to the natural dipeptide Phe-Gly.[14] An hPEPT1-mediated transport component was also demonstrated, which was in contrast to what was observed for hydroxyl containing amide bond isosteres.[14] Therefore, the ke-

* To whom correspondence should be addressed. Phone: +46-31-772-2894, fax: +46-31-772-3840, e-mail: luthman@chem.gu.se.
† Department of Medicinal Chemistry, University of Tromsø.
‡ The Danish University of Pharmaceutical Sciences.
⊥ Department of Chemistry, University of Tromsø.
§ Göteborg University.

10.1021/jm040780c CCC: $27.50 © 2004 American Chemical Society
Published on Web 08/10/2004

tomethylene amide bond replacement was considered a good starting point for a peptidomimetic prodrug approach targeting hPEPT1. BnOH was chosen as the model drug due to the inherent synthetic advantages, its ease of detection by UV and our previous experience with this type of model prodrugs.[8,9,15−20]

To investigate which position is best suited for drug attachment, we intended to link the model drug (BnOH) to all available positions that a natural dipeptide offers for an alcohol containing compound; the C-terminus (**1** and **2**), the R_2- (**3** and **4**), and the R_1-side chain positions (**5**) (Figure 1). We have earlier made thorough investigations of using the R_1-position as attachment point for different (model) drugs[11,15,20] and wanted to extend these studies to also involve attachments to the R_2- and C-terminal positions. Our previous studies have shown that the D-Asp(OcHx)-Ala model prodrug has affinity for hPEPT1,[15] and that the benzyl alcohol model prodrugs D-Glu(OBn)-Ala, D-Asp(OBn)-Ala and D-Ser(Bn)-Ala (ether linkage) are all substrates for hPEPT1.[8,9] Interestingly, the corresponding Asp(OBn)-Sar model compound seemed to be an inhibitor.[8] High hPEPT1-affinities have also been found for Glu-Sar ester prodrugs of acyclovir and the model compound thymine (ester linkage via a 1-(2-hydroxyethyl) spacer) whereas the corresponding D-Glu-Ala derivatives showed poor affinities.[11] However, based on intracellular accumulation studies, Glu[acyclovir]-Sar appears to be an inhibitor of hPEPT1.[21]

In the present study the model drug was linked to the different pro-moieties via an ester bond since this covalent linkage is generally more stable at slightly acidic pH than at slightly basic pH.[22] Therefore, a higher aqueous (chemical) stability of the prodrug is expected in the intestinal lumen than after passage across the brush border membrane. At the same time the linkage is bioreversible since it is liable to enzyme-catalyzed hydrolysis (i.e. esterases) once in the brush border membrane or the systemic circulation.

To provide "handles" for drug attachment in the R_1- and R_2-positions, a carboxylic acid functionality had to be introduced in the pro-moiety. Since the basic idea for this kind of prodrug is to mimic a natural dipeptide, Glu and Asp side chains were the two alternatives. As mentioned above, promising pro-moieties based on stabilized dipeptides (containing D-amino acids or *N*-methylated amide bonds) with both Glu and Asp in the R_1-position have earlier been investigated by our research groups,[9,20] but no unambiguous conclusion of which of these that is the most advantageous for binding and transport has yet been reached. We have earlier reported that model prodrugs based on stabilized dipeptides with Asp(OBn) side chains in the R_1-position were less stable than the corresponding Glu(OBn) derivatives,[19] but as this was a result of intramolecular cyclization due to attack from the amide NH-group, this effect is not likely to apply to ketomethylene isosteres. Due to the increased synthetic complexity of peptidomimetics (compared to amino acid coupling), the Asp side chain (CH_2COOH) was chosen in this study mainly because of the synthetic feasibility of such derivatives (see Chemistry section).

Considering our previous synthetic experience with Phe-Gly peptidomimetics, and especially the encouraging results from the biological investigations of the Phe-Gly ketomethylene isostere,[14] this derivative was a natural starting point for the pro-moiety design. But indications from the literature on the beneficial effects on affinity of an N-terminal valine residue[6,23,24] led us to extend the series of compounds from the phenylalanine-based compounds (**1** and **3**) to also include the valine analogues (**2** and **4**). This would enable a direct comparison of effects due to different R_1 side chains not taking direct part in the attachment of the model drug, providing further structural information about the hPEPT1 binding site.

Scheme 1

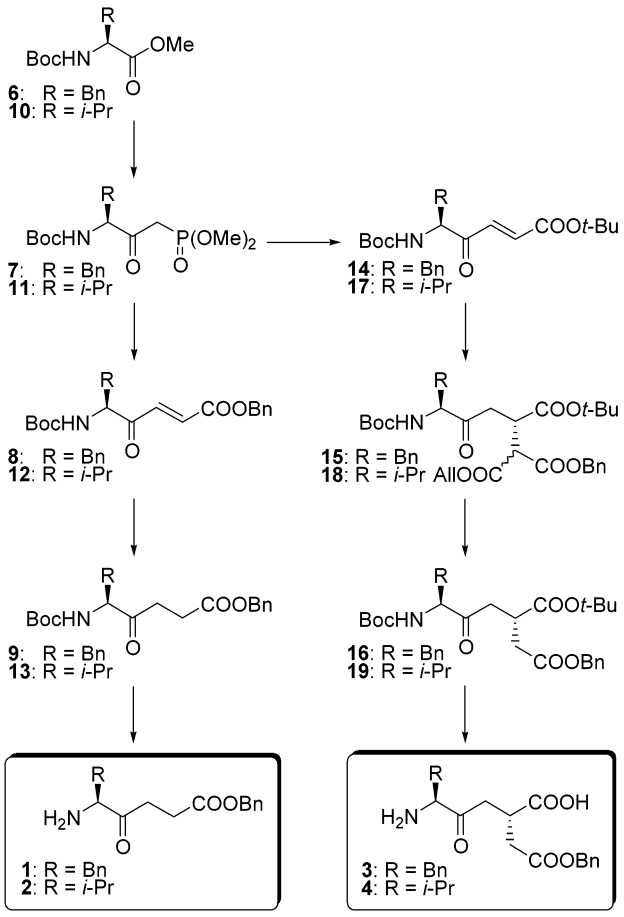

Results and Discussion

Chemistry. To obtain compounds with L-stereochemistry of the side chains, the synthetic strategy had to be designed accordingly, enabling all five compounds to be synthesized in a stereoselective manner. The synthetic strategy for **1**−**4** is outlined in Scheme 1. The syntheses of the key intermediates **8**,[25] **12**,[25] and **14**[26] have been described earlier. Selective double bond reduction of **8** and **12** in the presence of the benzyl ester was achieved using Wilkinson's catalyst under H_2-atmosphere[27,28] to give **9** and **13**, respectively. To introduce the L-Asp side chain in the R_2-position compounds **16** and **19** were synthesized via a diastereoselective Michael addition of the anion of allyl benzyl malonate to the unsaturated *tert*-butyl esters **14** and **17**, respectively, followed by deallylation and decarboxylation. The Michael reaction has earlier been investigated by Deziel et al.[25] who reported the highest

Scheme 2

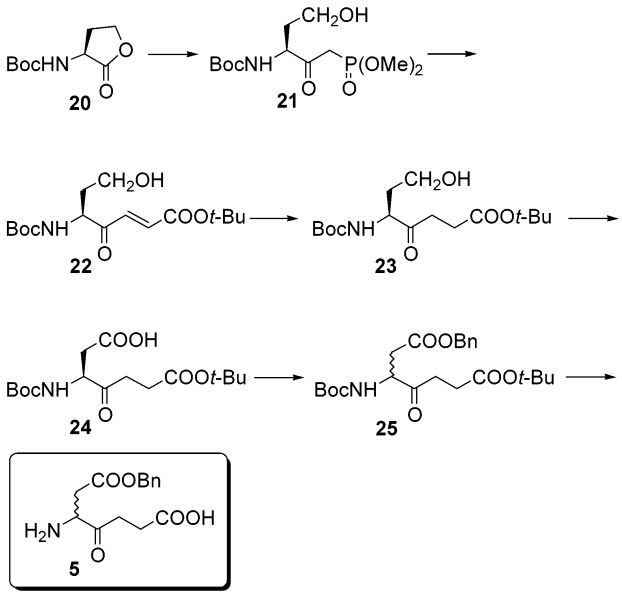

diastereoselectivity in the addition of the anion of allyl *tert*-butyl malonate to unsaturated γ-keto benzyl esters using NaH as base and THF as solvent at −78 °C. The Michael additions to **14** and **17** were therefore carried out analogously and were shown to be both regio- and stereoselective. The diastereomeric ratios were >80:20 for both compounds, assessed by ^{1}H NMR spectroscopy of the diastereomeric mixture of **16** and **19** and their (3*R*)-epimers and by analytical HPLC of crude **3** and **4** after deprotection.

The synthetic strategy for **5** is outlined in Scheme 2. Initial attempts to make the phosphonates from Boc-Glu(OBn)-OMe or Boc-Glu-OMe, analogously to the synthesis of **7**, were unsuccessful. For Boc-Glu(OBn)-OMe this could be due to an unselective attack of the phosphonate anion on the two ester functionalities. No reaction was observed for Boc-Glu-OMe, probably due to electrostatic repulsion from the deprotonated carboxylic acid.

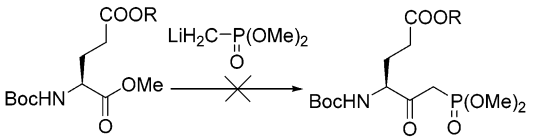

Instead, an alternative approach to the R_1-benzylated Asp-derivative was undertaken. Reaction of the phosphonate anion on the *N*-Boc protected lactone **20**, synthesized from the commercially available (*S*)-α-amino-γ-butyrolactone, provided the phosphonate **21**, which was converted to the unsaturated ketoester **22** using the standard Horner−Wadsworth−Emmons reaction. Subsequent catalytic hydrogenation using H_2/Pd in EtOAc gave the saturated analogue **23**. The primary alcohol was then oxidized with PDC in DMF[29] to give the desired carboxylic acid (aspartate side chain) **24**, which was finally benzylated using Cs_2CO_3 and benzyl bromide[30] to afford the diester **25**. This benzylation procedure is reported to be a mild method for esterification of amino acids and peptides,[30] but surprisingly the optical activity of **25** was lost during this reaction. The suspected racemization was confirmed after catalytic hydrogenation of **25**, which gave racemic **24**. However, due to the low chemical stability of the final racemic product **5** (see below), no further attempts were made to synthesize the pure L-enantiomer.

Selective *N*-Boc deprotection of **9** and **13** using HCl(g) in EtOAc gave the hydrochloride salts of **1** and **2**, while selective deprotection of the *N*-Boc and C-terminal *tert*-butyl ester of **16**, **19** and **25**, in the presence of the benzyl ester, was achieved with TFA in CH_2Cl_2, affording the trifluoroacetate salts of **3**−**5** (Schemes 1 and 2). Pure **3** and **4** were obtained by semipreparative reversed phase HPLC.

Chemical and Biological Stability of 1−5. It is evident that the stability of the prodrug is crucial for hPEPT1-mediated drug transport, as the prodrug must be sufficiently stable to survive the gastrointestinal environment, and at the same time be sufficiently labile to release the drug once it reaches the systemic circulation. Another important aspect of stability studies is to verify that the compounds are stable enough to make sound interpretations of data from in vitro assays, such as the Caco-2 cell assay used in this study. Hence, the chemical and biological stabilities of **1**−**5** were assessed by stability studies in buffer in the absence and presence of Caco-2 cells, respectively.

A. Chemical Stability Studies. The chemical stabilities of the model prodrugs **1**−**5** were investigated in both apical (pH 6.0) and basolateral (pH 7.4) transport buffers at 37 °C (Table 1). It was observed that compounds **1**−**5** all as expected were more stable at pH 6.0 than at 7.4 (maximum $p = 0.0056$). This effect was most pronounced for compounds **1** and **2**, being 11−12 times more stable at pH 6.0 than at 7.4, whereas **3**−**5** were 3−5 times more stable at the lower pH. When comparing the Phe- and Val-derivatives, compounds **2** and **4** were 2−3 times more stable than their corresponding Phe-derivatives **1** and **3** at either pH value (maximum $p = 0.007$). In terms of absolute values, **4** was the most stable compound at either pH value, whereas **5** was the most unstable compound at either pH value. It was also observed that the two Val-derivatives (**2** and **4**) were the most stable compounds at pH 6.0, while the two R_2-benzylated compounds (**3** and **4**) were the most stable at pH 7.4.

B. Biological Stability Studies. To assess the influence of enzyme-catalyzed hydrolysis of the compounds, stability studies in buffer in the presence of Caco-2 cells were carried out by investigating the amount of intact compound remaining on the apical side of the Caco-2 cell monolayers after the 2 h transport experiments (see below) for all compounds (Table 2). When comparing these results with the expected amount remaining in buffer (pH 6) after 2 h, calculated from the k_{obs} values obtained from the chemical stability studies, a significant decrease was observed for **1** and **2**. However, for the Asp(OBn) derivatives **3**−**5** there was no significant difference in the degradation in the absence or presence of Caco-2 cells. These results suggest the involvement of esterases in the degradation of **1** and **2**;[31] thus, it seemed as the C-terminal esters were more prone to enzymatic hydrolysis than the Asp(OBn) esters in the R_1- or R_2-positions. Overall, the results in Tables 1 and 2 indicated a sufficient stability

Table 1. Estimated Rate Constants and Half-Lives (±SD) for Chemical Degradation of Compounds **1**−**5** in Transport Buffers (pH 6.0 and 7.4) at 37 °C, Studied for Several Half-Lives or over a 48-h Period for Slower Degradations ($n = 3$)[a]

	pH 6.0[b]		pH 7.4[b]	
compound	k_{obs} (min^{-1})	$t_{1/2}$ (min)	k_{obs} (min^{-1})	$t_{1/2}$ (min)
1	$2.5 (\pm 0.1) \times 10^{-4}$	2803 ± 131	$2.7 (\pm 0.2) \times 10^{-3}$	255 ± 20
2	$8.4 (\pm 1.8) \times 10^{-5}$	8529 ± 1943	$9.7 (\pm 1.3) \times 10^{-4}$	721 ± 96
3	$1.8 (\pm 0.5) \times 10^{-4}$	4085 ± 928	$5.9 (\pm 0.4) \times 10^{-4}$	1171 ± 81
4	$6.1 (\pm 0.3) \times 10^{-5}$	11381 ± 560	$2.7 (\pm 0.1) \times 10^{-4}$	2591 ± 78
5	$3.5 (\pm 0.2) \times 10^{-3}$	200 ± 9	$1.04 (\pm 0.03) \times 10^{-2}$	67 ± 2

[a] Assessed by HPLC, see Experimental Section. [b] For buffer composition, see Experimental Section.

Table 2. Remaining Amount (%) of **1**−**5** after 120 min at 37 °C, pH 6, in the Absence and Presence of Caco-2 Cells

compound	buffer[a]	Caco-2[b]
1	97	2.2 ± 2.2
2	99	48 ± 1.3
3	98	100[c]
4	99	100[c]
5	66	73.3 ± 7.8

[a] Amount (%) remaining intact after 120 min in apical transport buffer (pH 6.0), calculated from k_{obs} (see Table 1). [b] Observed amount (%) remaining intact on the apical side of Caco-2 cell monolayers after the transport assay. [c] No detectable appearance of BnOH.

for all five compounds in the affinity studies (incubation time 5 min) but revealed that a careful examination of the data from the transepithelial transport assay (time course 120 min) was necessary for **1**, **2**, and **5**.

The bioreversible ester bond is a widely used linkage in prodrugs, especially in the lipophilic prodrug approach, benefiting from the difference in pH between the small intestine and the blood. This strategy is also applicable when designing a prodrug for hPEPT1, as the stability of all five compounds was higher at pH 6.0 than at 7.4. However, the results revealed large differences in chemical stability between the different compounds, indicating that some pro-moieties are better suited than others in this respect. It should be mentioned that the stability of an ester prodrug is highly dependent also on the structural properties of the attached drug[20] and is therefore likely to be different when a drug other than the model drug used in this study is attached.

Affinity and Transport Studies of 1−5 in Caco-2 Cell Monolayers. The synthesized derivatives **1**−**5** were tested for their affinity for hPEPT1 based on inhibition of [^{14}C]-Gly-Sar uptake using the Caco-2 cell assay as described earlier.[14] The transepithelial transport of **1**−**5** across Caco-2 monolayers, including uptake (intracellular accumulation), was also investigated. In these studies Gly-Sar was used as the reference compound, and mannitol as the marker of paracellular transport.

A. Affinity for hPEPT1. The affinities of **1**−**5** for hPEPT1 in confluent mature Caco-2 cell monolayers were determined by their ability to inhibit the transport of [^{14}C]-Gly-Sar, a standard substrate for hPEPT1. The results (Figure 2, Table 3) demonstrated that in the context of hPEPT1 all compounds had high affinities ($K_i < 1$ mM), and that PheΨ[$COCH_2$]Asp(OBn) (**3**) and ValΨ[$COCH_2$]Asp(OBn) (**4**) had the highest affinities, with K_i values of 68 and 19 μM, respectively. The differences in the K_i values for the Val-derivatives (**2** and **4**) and their corresponding Phe-derivatives (**1** and **3**, respectively) are statistically significant (Table 3).

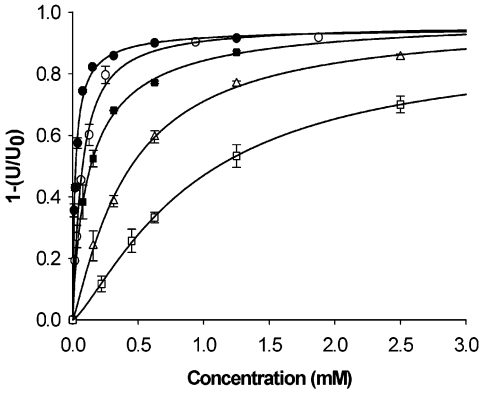

Figure 2. Inhibition of [^{14}C]-Gly-Sar uptake by **1** (□), **2** (■), **3** (○), **4** (●), and **5** (△) in Caco-2 cells. The lines describe the best fit to the experimentally obtained points using eq 1. Error bars represent SE.

Table 3. IC_{50} and K_i Values of **1**−**5** for hPEPT1 in Caco-2 Cells

compound	IC_{50} (μM)	K_i (μM)
1	915 ± 37	905
2	134 ± 13	133
3	69 ± 6	68
4	19 ± 2	19
5	422 ± 33	417

Using Student's *t*-test a significant difference in affinity between **1** and **2** was found ($p < 0.0001$, $n = 3$) and similarly a significant difference between **3** and **4** ($p = 0.0013$, $n = 3$).

B. Transepithelial Transport and Uptake Studies. As affinity studies only give information about binding to hPEPT1, transepithelial transport studies were subsequently carried out to investigate the overall transport across the Caco-2 cell monolayer. Additionally, the uptake, i.e., the amount of compound accumulated intracellularly after completion of the transport studies (2 h), was assessed to investigate the actual cellular accumulation mediated by hPEPT1. To demonstrate active transport, these experiments were carried out in the absence and presence (20-fold excess) of the hPEPT1 competitive inhibitor Gly-Pro.

The results from the transport experiments showed that **3**−**5** were transported across the Caco-2 cell monolayer (Figure 3). A significant reduction ($p < 0.05$, $n = 3$) in the flux of **3**−**5** was observed in the presence of Gly-Pro, indicating an hPEPT1-mediated transport component in the overall transepithelial transport of these three compounds. The same was observed for the reference compound Gly-Sar, confirming the involvement of hPEPT1. As there was no significant difference in the flux of the paracellular marker mannitol in the presence and absence of Gly-Pro (P_{app} values of $8.7 \pm 0.6 \times 10^{-7}$ and $9.4 \pm 0.2 \times 10^{-7}$ cm $\times$ s^{-1}, respectively, $n = 3$, $p > 0.05$), the changes in the flux of **3**−**5** were not likely to be an effect of decreased paracellular

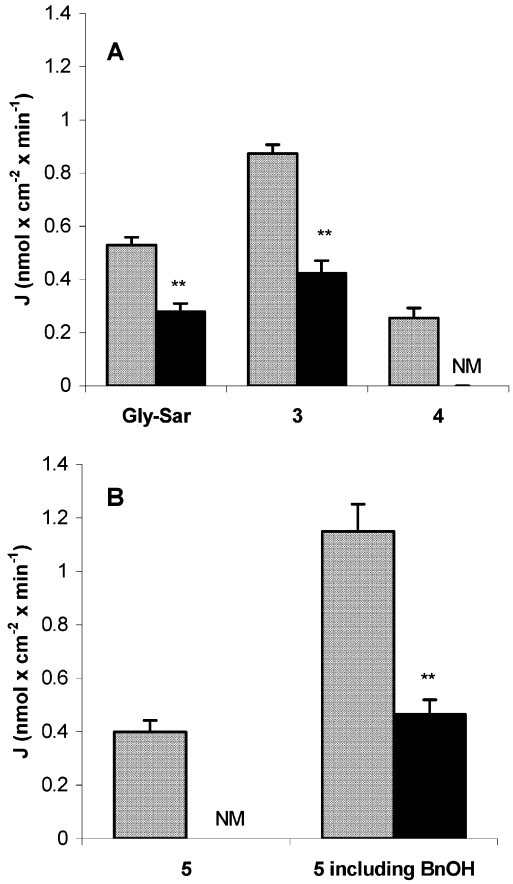

Figure 3. Transepithelial flux (J) of 1 mM compound across Caco-2 cell monolayers in the absence (gray) and in the presence (black) of 20 mM Gly-Pro. (A) Gly-Sar, **3** and **4**; (B) **5** and **5** including BnOH. NM: not measurable. Error bars represent SE. ** $p < 0.01$.

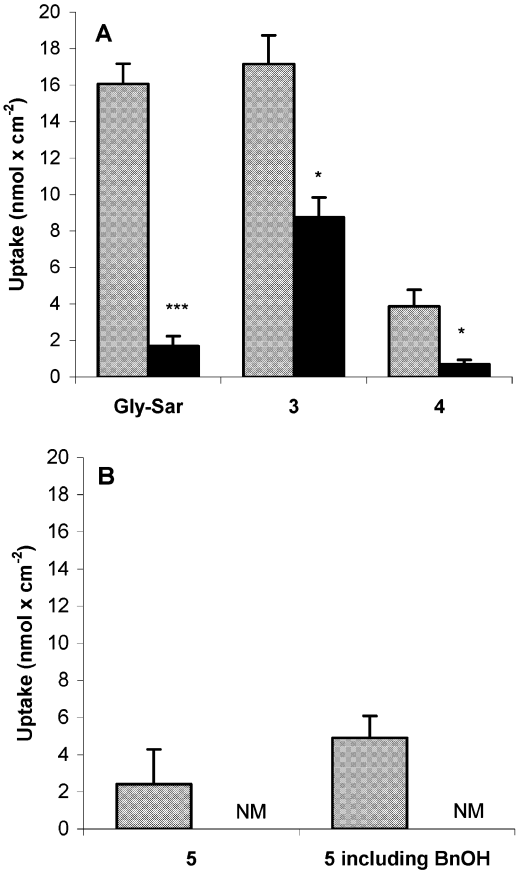

Figure 4. Intracellular uptake of 1 mM compound in Caco-2 cells in the absence (gray) and in the presence (black) of 20 mM Gly-Pro after 2 h. (A) Gly-Sar, **3** and **4**; (B) **5** and **5** including BnOH. NM: not measurable. Error bars represent SE. * $p < 0.05$ and *** $p < 0.001$.

transport. Also the uptake of **3**−**5** (Figure 4) was significantly different in the presence and absence of Gly-Pro, corroborating transcellular transport mediated by hPEPT1. A significant release of BnOH during the time course of the experiments (2 h) was observed for **5**, which could be expected from the chemical stability studies. The transepithelial transport of BnOH was relatively fast with a P_{app} value of $1.40 \pm 0.04 \times 10^{-4}$ cm $\times$ s^{-1}. This indicates that the apically released BnOH is transported across the Caco-2 cells, thereby contributing to the flux calculated for **5** including BnOH, as illustrated in Figure 3B. The flux for **5** is thus the difference in total transport of **5** and BnOH in the absence and presence of Gly-Pro (approximately 0.7 nmol $\times$ min^{-1} $\times$ cm^{-2}). For **3** and **4** no release of BnOH was observed, suggesting that not only the chemical stabilities of these two compounds, but also their biological stabilities, could be sufficient to warrant the use of these as pro-moieties in a prodrug approach targeting hPEPT1. Although the chemical stability of **1** and **2** was sufficient, the biological stability studies, i.e., in the presence of Caco-2 cells, showed that **1** and **2** were degraded during the course of the experiment. Thus, it was impossible to determine accurate flux values for **1** and **2**, although for **2** intact compound was observed basolaterally in the first sample ($t = 40$ min, results not shown). But as no compound was left at the end of the experiment ($t = 120$ min), a significant basolateral esterase activity was also evident. In the presence of 20 mM Gly-Pro intact **2** could not be detected, giving a weak indication that **2** in fact is a substrate for hPEPT1.

Structure−**Affinity Relationships for hPEPT1.** As the 3D structure of hPEPT1 not yet has been established, only indirect evidence for the transporter topology can be obtained, based on epitope tagging[32] and site-directed mutagenesis studies.[33−37] Thus, ligand based design is currently the only way to extract structure-affinity information for the transporter. The affinities of a large number of natural peptides have been determined, whereas the effects of modification of the side chains of natural peptides have been investigated to a lesser degree. Still, an interaction of the R_2 side chain with a proposed hydrophobic pocket has been suggested,[38] and studies have also indicated that substrates may interact with a hydrophobic pocket in the R_1-position.[20] A reasonable amount of data has been accumulated on the importance of the different functional groups in the peptide backbone, such as charged N- and C-termini and the carbonyl functionality of the N-terminal amino acid. Over the years several template models for hPEPT1 have been proposed, including a

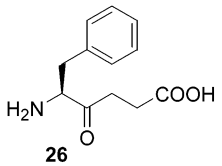

26

general model for both di- and tripeptides[38] based on molecular modeling of a diverse set of substrates/inhibitors. Recently a more detailed model for dipeptides and amino acid aryl amides based on CoMFA and CoMSIA was published.[39]

We have recently shown that the replacement of the enzymatically labile amide bond of Phe-Gly with the stable ketomethylene isostere (PheΨ[$COCH_2$]Gly, **26**) only reduced the apparent affinity for hPEPT1 2-fold (K_i values of 0.20 and 0.40 mM, respectively). The apparent affinity for rPEPT2 was not significantly changed, demonstrating that **26** is a high affinity ligand for both PEPT1 and PEPT2.[14] From Table 3 it is seen that the substitution of the R_1 benzyl side chain of **26** with the benzylated aspartate side chain of **5** had a negligible effect on the affinity for hPEPT1 (K_i values of 0.40 and 0.45 mM, respectively). The importance of a hydrophobic R_1-side chain has earlier been pointed out,[20] and it is likely that the phenyl ring in **5**, despite of the ester functionality, contributes in this respect, in the same way as the phenylalanine side chain does for **26**. This observation is also in agreement with earlier studies of R_1-benzylated stabilized Glu-Xaa and Asp-Xaa dipeptides showing high affinity for hPEPT1.[9,20]

The model prodrug **1** corresponds to the C-terminal benzyl ester of **26**, a modification that reduced the affinity for hPEPT1 approximately 2-fold. This is in agreement with earlier studies showing that an unsubstituted C-terminus is advantageous for binding to the transporter. It should also be mentioned that the solubility and/or dissolution rate of **1** in water was low, a problem that was overcome by addition of maximum 0.5−1.0% DMSO to the test medium. Even if this was the prodrug with lowest affinity in our series, a K_i value below 1 mM is still considered interesting.

Compound **2** is in effect the benzyl ester of ValΨ[$COCH_2$]Gly, but contrary to **1** this C-terminally benzylated compound has an improved affinity compared to **26** and an approximately 7-fold improvement in affinity compared to **1**. This is likely to be an effect of the isopropyl side chain of Val in the R_1-position, and it has been shown in several studies that Val in R_1 has an advantageous effect on binding compared to other amino acids.

The R_2-benzylated Xaa-Asp ketomethylene isosteres **3** and **4** are the two compounds with highest affinity in this series, with K_i values in the lower μM-range. This indicates a strong favorable effect of the benzylated aspartate side chain compared to the hydrogen of **26**. The substrate template of Bailey et al.[38] suggests that a hydrophobic R_2-group is an advantage, and in the same way as for **5** the phenyl ring of the benzyl alcohol contributes in this respect. But as an Asp(OBn) side chain in R_2 has a much bigger impact on the K_i value than the same substitution in R_1, these results indicate that there are stronger hydrophobic interactions with residues in the R_2 binding site and probably also less restriction in size. A significant increase in affinity by substitution of a benzyl group (Phe) with an isopropyl group (Val) in the R_1-position is also observed for **3** and **4**, here resulting in an approximate 3-fold improvement in affinity for the Val-derivative.

Thus, the affinity studies demonstrate that the isopropyl side chain of Val in the R_1-position has a beneficial effect on affinity compared to Phe. There are two possible explanations for this observation: the isopropyl group contributes to the stabilization of the bioactive conformation, or the binding site of hPEPT1 has a preference for the isopropyl group, indicating an especially favorable interaction with residues in the binding site of hPEPT1. It is also seen that modifications in the R_2-position are better tolerated, and even seem advantageous, compared to the R_1-position and the C-terminus.

Structure−Transport Relationships for hPEPT1. The fact that a significant amount of **1** and **2** was degraded in the apical compartment during the assay, and probably also intracellularly and basolaterally, made interpretations of the transport of the intact compound impossible.

In terms of absolute values compound **3** showed the highest flux and uptake; however, flux and uptake of **3** were also measurable in the presence of Gly-Pro. Due to the two phenyl rings in **3**, this compound is more hydrophobic than the two other zwitterionic compounds **4** and **5**, suggesting that the flux and uptake which was not inhibited by Gly-Pro are contributions from a passive transcellular transport component.

Both flux and uptake were similar for compounds **4** and **5**, and as no flux was observed in the presence of Gly-Pro, a purely carrier-mediated transpithelial transport for these two compounds was indicated. For compound **5**, a significant amount of the model drug BnOH was detected in the basolateral compartment, both in the presence and absence of inhibitor. As no intact compound could be detected intracellularly or basolaterally when Gly-Pro was added, the basolateral presence of BnOH under these conditions indicates apical hydrolysis of the parent compound followed by passive transpithelial transport of BnOH. The increase in intracellular and basolateral amount of BnOH in absence of Gly-Pro indicates that both apical, intracellular, and basolateral hydrolysis of the parent compound take place during the transport experiment.

Overall, the transport and uptake experiments showed that **3**−**5** are substrates for hPEPT1. The transepithelial flux of **3**−**5** is comparable to the flux measured for orally active β-lactam antibiotics across Caco-2 cells,[4] which further indicate that dipeptidic ketomethylene isosteres constitute a promising class of compounds for development of pro-moieties for optimizing oral bioavailability by targeting hPEPT1.

Conclusions

Chemical and biological investigations of a series of structurally related benzyl alcohol model prodrugs based on the dipeptide ketomethylene isostere have provided important information on the structure−affinity and structure−transport relationships for hPEPT1 and also on the stability of the ester prodrug linkage. The affinity studies showed that introduction of the isopropyl side chain of Val in the R_1-position is advantageous for binding affinity, and also for stability, compared to the benzyl side chain of Phe. It has also been demonstrated that in terms of affinity drug attachment in the R_2-position is better tolerated, and even seem advantageous, compared to the R_1-position or the C-terminus.

As the degradation rates for **1** and **2** were much higher than what were observed in the stability studies in buffer, the involvement of enzymes, i.e., esterases, was indicated. Regarding the use of the ester linker in a potential prodrug, the assessment of the influence of enzymes (i.e. esterases) on the stability of the prodrug is needed to enable translation of data into an in vivo situation. The results of this study imply that PheΨ-[$COCH_2$]Asp and ValΨ[$COCH_2$]Asp are particularly promising pro-moieties for a prodrug approach aimed at increasing oral bioavailability via hPEPT1-mediated transport, and testing of this hypothesis using poorly absorbable drugs is presently ongoing in our laboratory.

Experimental Section

Chemistry. General. Starting materials and reagents were purchased from Sigma, Fluka, Aldrich, Senn Chemicals, and Merck KGaA and were used as received. ^{1}H and ^{13}C NMR spectra were recorded on a Varian Mercury Plus spectrometer operating at 400 and 100 MHz, respectively. Chemical shifts are given relative to the solvent signal (δ 7.26 and δ 77.0 for $CDCl_3$, and δ 3.49 and δ 49.0 for CD_3OD, respectively). TLC was run on silica gel coated aluminum sheets (silica gel 60 F_{254}, Merck), with visualization by UV detection and/or 5% phosphomolybdic acid hydrate (PMA) in EtOH, followed by heating. Flash chromatography was performed on silica gel (silica gel 60 (0.040−0.063 mm), Merck) under nitrogen pressure, if not stated otherwise. THF was distilled from Na/benzophenone ketyl. Other solvents were of analytical or synthetic grade and were used without further purification. Melting points were taken with a Büchi Melting Point B-540 apparatus and are uncorrected. Optical activity was measured using a Perkin-Elmer 241 Polarimeter. Elemental analyses were done by Mikro Kemi AB, Uppsala, Sweden. In HPLC a Waters 510 pump, a Waters 2487 Dual λ Absorbance Detector operating at 254 nm, and a Varian 4400 Integrator were used. Reversed phase analytical chromatography of crude **3** and **4** was performed on a Symmetry C18, 5 μm, 3.9 × 150 mm analytical column from Waters (isocratic: 28% CH_3CN, 0.1% TFA; flow rate 1 mL/min). Purification of compounds **3** and **4** by reversed phase preparative chromatography was performed on a Prep Nova-Pak HR C18 6 μm 60 Å 25 ×100 mm column from Waters (isocratic: **3**: 34% CH_3CN, 0.1% TFA, **4**: 28% CH_3CN, 0.1% TFA; flow rate 7.0 mL/min). The syntheses of **8**,[25] **11**,[25] **12**,[25] **7**,[26] **14**,[26] **20**,[40] and allyl benzyl malonate[41] have been described earlier.

Dimethyl [(3*S*)-3-[*N*-(*tert*-Butoxycarbonyl)amino]-4-methyl-2-oxopentyl]phosphonate (11). Compound **11** was synthesized in 84% yield (4.21 g) from **10** (3.02 g, 13.06 mmol) according to a literature procedure for the synthesis of **7**.[26] Compound **11** was isolated as a colorless oil. For spectroscopical data on **11**, see ref 25.

Benzyl (5*S*)-5-[*N*-(*tert*-Butoxycarbonyl)amino]-4-oxo-6-phenyl-(*E*)-2-hexenoate (8). Compound **8** was synthesized in 58% yield (972 mg) from **7** (1.60 g, 4.31 mmol), according to a literature procedure for the synthesis of **14**,[26] using benzyl glyoxylate instead of *tert*-butyl glyoxylate. Compound **8** was isolated as a yellow oil. For spectroscopical data on **8**, see ref 25.

Benzyl (5*S*)-5-[*N*-(*tert*-Butoxycarbonyl)amino]-6-methyl-4-oxo-(*E*)-2-heptenoate (12). Compound **12** was synthesized in 47% yield (211 mg) from **11** (420 mg, 1.30 mmol), according to a literature procedure for the synthesis of **14**,[26] using benzyl glyoxylate instead of *tert*-butyl glyoxylate. Compound **12** was isolated as a light yellow oil. For spectroscopical data on **12**, see ref 25.

Benzyl (5*S*)-5-[*N*-(*tert*-Butoxycarbonyl)amino]-6-methyl-4-oxo-heptanoate (13) (General Procedure for the Double Bond Reduction of α,β-Unsaturated γ-Keto Benzyl Esters). Wilkinson's catalyst ($Ph_3P)_3RhCl$ (82 mg, 0.1 equiv) and **12** (211 mg, 0.61 mmol) were dissolved in benzene (20 mL) under inert conditions. The reaction was stirred under H_2 atmosphere at 50 °C for 20−24 h. The solvent was evaporated under reduced pressure, and diethyl ether was added to precipitate the catalyst. The suspension was filtered through a short silica gel column (diethyl ether), and the filtrate was concentrated under reduced pressure. The residue was purified by flash chromatography on basic Al_2O_3 using diethyl ether as eluent to afford **13** (112 mg, 56%) as a colorless oil: $[\alpha]_D$ +8.0° (*c* 1.08, $CHCl_3$); ^{1}H NMR ($CDCl_3$) δ 7.42−7.32 (m, 5H), 5.16 (br s, 1H), 5.14 (s, 2H), 4.36−4.28 (m, 1H), 3.00−2.90 (m, 1H), 2.84−2.59 (m, 3H), 2.30−2.19 (m, 1H), 1.47 (s, 9H), 1.03 (d, 3H, J = 6.4 Hz), 0.81 (d, 3H, J = 6.8 Hz); ^{13}C NMR ($CDCl_3$) δ 207.9, 172.4, 156.0, 135.8, 128.6 (2 C:s), 128.3, 128.2 (2 C:s), 79.7, 66.6, 63.9, 35.4, 30.3, 28.3 (3 C:s), 27.7, 19.9, 16.7.

Benzyl (5*S*)-5-[*N*-(*tert*-Butoxycarbonyl)amino]-4-oxo-6-phenyl-hexanoate (9). Reduction of **8** (267 mg, 0.56 mmol) was performed as described above to afford 129 mg of **9** (48%) as a white solid: Mp 87.5−89.5 °C; $[\alpha]_D$ +5.2° (*c* 1.0, $CHCl_3$); ^{1}H NMR ($CDCl_3$) δ 7.43−7.17 (m, 10H), 5.15 (s, 2H), 5.10 (d, 1H, J = 7.6 Hz), 4.57 (dd, 1H, 14.2, 7.0 Hz), 3.14 (dd, 1H, 14.2, 6.2 Hz), 2.96 (dd, 1H, 14.2, 7.0 Hz), 2.83−2.76 (m, 2H), 2.70−2.64 (m, 2H), 1.43 (s, 9H); ^{13}C NMR ($CDCl_3$) δ 207.5, 172.4, 155.3, 136.3, 135.8, 129.3 (2 C:s), 128.7 (2 C:s), 128.6 (2C:s), 128.3, 128.2 (2 C:s), 127.0, 80.0, 66.6, 60.2, 37.5, 35.1, 28.3 (3 C:s), 27.8.

***tert*-Butyl (5*S*)-5-[*N*-(*tert*-Butoxycarbonyl)amino]-6-methyl-4-oxo-(*E*)-2-heptenoate (17).** Compound **17** was synthesized in 60% yield (321 mg) from phosphonate **11** (527 mg, 1.63 mmol), as described in the literature for the synthesis of **14**.[18] Compound **17** was isolated as a light yellow oil: $[\alpha]_D$ +63.8° (*c* 0.93, $CHCl_3$); ^{1}H NMR ($CDCl_3$) δ 7.13 (d, 1H, J = 16.0 Hz), 6.75 (d, 1H, J = 16.0 Hz), 5.20 (d, 1H, J = 8.4 Hz), 4.56 (dd, 1H, J = 8.4, 4.0 Hz), 2.25−2.10 (m, 1H), 1.53 (s, 9H), 1.47 (s, 9H), 1.05 (d, 3H, J = 7.2 Hz), 0.81 (d, 3H, J = 6.8 Hz); ^{13}C NMR ($CDCl_3$) δ 198.6, 164.4, 155.8, 136.0, 134.2, 82.2, 79.9, 63.2, 30.2, 28.3 (3 C:s), 28.0 (3 C:s), 19.9, 16.7.

Allyl Benzyl Malonate. A solution of benzyl acetate (1.20 g, 8.0 mmol) in dry THF (25 mL) was cooled to −78 °C, and LiHMDS (1.0M in THF) (8.0 mL, 8.0 mmol) was added dropwise over a period of 10 min. The reaction mixture was stirred at −78 °C for 1 h before allylchloroformate (1.49 g, 12.4 mmol) dissolved in THF (10 mL) was added by needle transfer over 15 min. The mixture was stirred at −78 °C for 2 h. The reaction was quenched by addition of 10% citric acid (10 mL). The resulting solution was extracted with diethyl ether (3 × 50 mL). The combined organic phase was washed with brine, dried over $MgSO_4$, and concentrated to give a yellow oil. The residue was purified by flash chromatography [pentane:diethyl ether 9:1] to afford 1.30 g allyl benzyl malonate (68%) as a colorless oil. For spectroscopical data on the product, see ref 41.

Benzyl (3*S*,6*S*)-3-(*tert*-Butoxycarbonyl)-6-[*N*-(*tert*-butoxycarbonyl)amino]-7-methyl-5-oxo-octanoate (19) (General Procedure for the Michael Reaction, Deallylation, and Decarboxylation). (a) Sodium hydride (60% in mineral oil, 0.45 mmol, 18 mg) was added to a solution of allyl benzyl malonate (234 mg, 1.00 mmol) in THF (10 mL). After the gas evolution ceased, the reaction mixture was cooled to −78 °C and **17** (262 mg, 0.80 mmol) dissolved in THF (10 mL) was added dropwise over a period of 15 min. The mixture was stirred at −78 °C for 2.5 h when the reaction was quenched with 10% citric acid (10 mL). Water (30 mL) was added, and the mixture was extracted with diethyl ether (3 × 30 mL). The combined organic phase was washed with brine and dried over $MgSO_4$. The solvent was evaporated under reduced pressure to afford 419 mg of crude **18** (93%) as a colorless oil that was used in the next step without further purification or characterization.

(b) A solution of crude **18** (419 mg, 0.75 mmol) in toluene (5 mL) was added during 5 min to a solution of the catalyst Pd($PPh_3)_4$ (45 mg, 0.05 equiv) and pyrrolidine (1.38 mmol, 115 μL) in toluene (10 mL). The reaction was stirred at room temperature for 7 h. The mixture was diluted with EtOAc (30 mL) and washed with 0.1 M HCl, water, and brine. The organic phase was dried over $MgSO_4$ and concentrated. The crude

deallylated product was used in the next step without further purification or characterization.

(c) The crude carboxylic acid was dissolved in xylene (15 mL) and decarboxylated on heating at 130 °C for 4 h. The mixture was concentrated, and the residue was purified by flash chromatography on silica gel [pentane:diethyl ether 3:1] to afford 226 mg of **19** and its 3*R*-epimer (59% from **17**) as a colorless oil: ^{1}H NMR ($CDCl_3$) (major isomer) δ 7.40−7.30 (m, 5H), 5.20−5.10 (m, 3H), 4.25 (dd, 1H, J = 8.8, 4.0 Hz), 3.26−3.20 (m, 1H), 3.03 (dd, 1H, J = 18.4, 6.8 Hz), 2.77−2.68 (m, 2H), 2.59 (dd, 1H, J = 16.4, 7.2 Hz), 2.24−2.12 (m, 1H), 1.45 (s, 9H), 1.41 (s, 9H), 1.03 (d, 3H, J = 6.4 Hz), 0.78 (d, 3H, J = 6.8 Hz); ^{13}C NMR (major isomer) ($CDCl_3$) δ 207.3, 172.4, 171.4, 155.9, 135.7, 128.6 (2 C:s), 128.4 (2 C:s), 128.36, 81.2, 79.7, 66.6, 63.8, 41.6, 37.0, 35.6, 30.1, 28.3 (3C:s), 27.9 (3C:s), 20.0, 16.5.

Benzyl (3*S*,6*S*)-3-(*tert*-Butoxycarbonyl)-6-[*N*-(*tert*-butoxycarbonyl)amino]-5-oxo-7-phenyl-heptanoate (16). Crude **15** (453 mg, 90%, colorless oil) was synthesized from **14** (310 mg, 0.83 mmol) as described above for crude **18**. Subsequent deallylation and decarboxylation afforded 228 mg of **16** and its 3*R*-epimer (59% from **14**) as a light yellow oil: ^{1}H NMR (major isomer) ($CDCl_3$) δ 7.42−7.16 (m, 10 H), 5.15 (app d, 2H), 5.06 (d, 1H, J = 8.0 Hz), 4.51 (dd, 1H, J = 14.2, 7.0 Hz), 3.26−3.19 (m, 1H), 3.14 (dd, 1H, J = 14.0, 6.0 Hz), 3.0−2.88 (m, 2H), 2.78−2.68 (m, 2H), 2.57 (dd, 1H, J = 16.8, 6.0 Hz), 1.42 (s, 18H); ^{13}C NMR (major isomer) ($CDCl_3$) δ 206.9, 172.4, 171.5, 155.2, 136.3, 135.7, 129.4, 129.4 (2 C:s), 128.7 (2 C:s), 128.6 (2 C:s), 128.4 (2 C:s), 127.0, 81.2, 80.0, 66.5, 60.1, 41.3, 37.3, 37.0, 35.4, 28.3 (3 C:s), 27.9 (3 C:s).

***N*-(*tert*-Butoxycarbonyl)-L-homoserine Lactone (20).** Triethylamine (835 μL, 6 mmol) was added to a suspension of (*S*)-α-amino-γ-butyrolactone hydrobromide (1.0 g, 5.5 mmol) in THF (10 mL) at 0 °C. A solution of di-*tert*-butyl dicarbonate (1.32 g, 6 mmol) in THF (5 mL) was added, and the reaction was stirred for 30 min at 0 °C and then overnight at room temperature. THF was removed under reduced pressure, and H_2O (25 mL) was added. The aqueous phase was adjusted to pH ∼5 with 10% aqueous citric acid and extracted with EtOAc (3 × 30 mL). The organic phase was dried ($MgSO_4$) and the solvent removed under reduced pressure to give 1.09 g (98%) of **20** as a yellow solid. For spectroscopical data on **20**, see ref 40.

Dimethyl [(3*S*)-3-[*N*-(*tert*-Butoxycarbonyl)amino]-5-hydroxy-2-oxopentyl]-phosphonate (21). Dimethyl methylphosphonate (1.6 mL, 15.0 mmol) was dissolved in THF (30 mL), and the solution was cooled to −78 °C under an atmosphere of nitrogen. Butyllithium (1.6 M in hexane) (9.25 mL, 14.8 mmol) was added in one portion, and the solution was stirred for 30 min before **20** (1.01 g, 5.0 mmol) dissolved in THF (25 mL) was added by a double-ended needle. After stirring for 1 h at −78 °C, 10% citric acid (16 mL) was added, and the cooling bath was removed. When the solution had reached room temperature, water (15 mL) was added and the solution was extracted with diethyl ether (2 × 20 mL). The combined ethereal extracts were washed with water (20 mL) and brine (20 mL), dried ($MgSO_4$), and concentrated. Purification of the residue by flash chromatography on silica gel using diethyl ether as eluent afforded **21** (740 mg, 48%) as a colorless oil that was used in the subsequent reaction without further purification or characterization.

***tert*-Butyl (5*S*)-5-[*N*-(*tert*-Butoxycarbonyl)amino]-7-hydroxy-4-oxo-(*E*)-2-heptenoate (22).** Phosphonate **21** (740 mg, 2.4 mmol) and lithium chloride (103 mg, 2.4 mmol) were dissolved in acetonitrile (20 mL), and the solution was cooled to 0 °C in an ice bath. Triethylamine (335 μL, 2.4 mmol) was added, followed by *tert*-butyl glyoxylate (0.57 g, 4.3 mmol) dissolved in acetonitrile (16 mL). Stirring was continued for 1 h at 0 °C after which 10% citric acid (50 mL) was added. The solution was extracted with diethyl ether (2 × 100 mL), and the combined ethereal extracts were washed with water (50 mL) and brine (50 mL) before drying ($MgSO_4$) and concentration. Purification of the residue by flash chromatography on silica gel [pentane:diethyl ether 1:1] afforded **22** (420 mg, 53%) as a colorless oil that was used without further characterization.

***tert*-Butyl (5*S*)-5-[*N*-(*tert*-Butoxycarbonyl)amino]-7-hydroxy-4-oxo-heptanoate (23).** Compound **22** (420 mg, 1.28 mmol) and Pd(C) (10%, 47 mg) were placed in a round-bottomed flask and EtOAc (25 mL) was added before the flask was fitted with a hydrogen-filled balloon. The mixture was stirred at room temperature and was monitored by TLC (SiO_2, diethyl ether:pentane, 1:1), and after 3 h no starting material could be detected. Filtration through Celite and solvent removal under reduced pressure left an oil that was filtered through a silica gel column using diethyl ether as eluent to afford **23** (250 mg, 59%) as a colorless oil that was used in the next step without further purification or characterization.

(3*S*)-6-(*tert*-Butoxycarbonyl)-3-[*N*-(*tert*-butoxycarbonyl)-amino]-4-oxo-hexanoic Acid (24). Compound **23** (250 mg, 0.75 mmol) was dissolved in freshly distilled DMF (3.5 mL) and solid pyridinium dichromate (1.41 g, 3.7 mmol) was added in one portion. The reaction was monitored by TLC (SiO_2, diethyl ether) and after 2.5 h the reaction was quenched by addition of saturated aqueous $NaHCO_3$ (25 mL). The mixture was extracted once with pentane and the aqueous phase was acidified by addition of concentrated HCl. The solution was extracted with diethyl ether (2 × 20 mL), dried ($MgSO_4$), and concentrated to afford **24** (161 mg, 62%) as a light yellow oil: $[\alpha]_D$ −10.5° (*c* 0.82, $CHCl_3$); ^{1}H NMR ($CDCl_3$) δ 5.71 (d, 1H, J = 8.8 Hz), 4.50−4.48 (m, 1H), 3.05 (dd, 1H, J = 17.6, 4.4 Hz), 2.94−2.80 (m, 3H), 2.54 (t, 2H, J = 6.4 Hz), 1.48 (s, 9H), 1.44 (s, 9H); ^{13}C NMR ($CDCl_3$) δ 207.0, 175.8, 172.1, 155.6, 80.9, 80.5, 55.8, 35.5, 33.8, 29.3, 28.3 (3 C:s), 28.0 (3 C:s).

Benzyl (3*R*/*S*)-6-(*tert*-Butoxycarbonyl)-3-[*N*-(*tert*-butoxycarbonyl)amino]-4-oxo-hexanoate (25). Compound **24** (112 mg, 0.33 mmol) was dissolved in MeOH (2 mL), and H_2O (200 μL) was added. Cs_2CO_3 (20% aqueous solution) was added until pH ∼8 (pH paper). After evaporation to dryness under reduced pressure, DMF (1.2 mL) was added and the solvent was removed at the pump (water bath kept at 45 °C). DMF (1.2 mL) was once more added and removed at the pump to leave a semisolid yellowish material. DMF (1.2 mL) and benzyl bromide (0.38 mmol, 45 μL) were added, and the solution was stirred at room temperature for 6 h. Solvents were removed under reduced pressure and H_2O (5 mL) was added. The aqueous solution was extracted with EtOAc (2 × 5 mL), and the combined organic extracts were dried ($MgSO_4$) and concentrated to afford **25** (102 mg, 72%) as a light yellow oil: ^{1}H NMR ($CDCl_3$) δ 7.42−7.32 (m, 5H), 5.67 (d, 1H, J = 8.4 Hz), 5.14 (dd, 2H, J = 14.4, 12.4 Hz), 4.56−4.52 (m, 1H), 3.04 (dd, 1H, J = 17.2, 5.2 Hz), 2.94−2.78 (m, 3H), 2.54 (app t, 2H), 1.48 (s, 9H), 1.46 (s, 9H); ^{13}C NMR ($CDCl_3$) δ 207.0, 171.8, 171.3, 155.4, 135.4, 128.6 (2 C:s), 128.4, 128.3 (2 C:s), 80.7, 80.3, 66.9, 56.0, 35.7, 34.0, 29.2, 28.3 (3 C:s), 28.1 (3 C:s).

Benzyl (5*S*)-5-Amino-4-oxo-6-phenyl-hexanoate (1). Compound **9** (53 mg, 0.13 mmol) was dissolved in EtOAc (5 mL) saturated with HCl(g). The mixture was stirred at room temperature for 15 min. Diethyl ether (15 mL) was added, and the solution was concentrated under reduced pressure. This procedure was repeated three times. The residue was extracted with water (2 × 10 mL) and diethyl ether (10 mL). The aqueous phase was concentrated to afford 41 mg of **1** (92%) as a white solid: Mp 94−96 °C; $[\alpha]_D$ +17.3° (*c* 0.92, MeOH); ^{1}H NMR (CD_3OD) δ 7.44−7.32 (m, 10H), 5.15 (s, 2H), 4.56−4.48 (m, 1H), 3.39 (dd, 1H, J = 14.4, 6.0 Hz), 3.03 (dd, 1H, J = 14.4, 8.0 Hz), 2.95−2.85 (m, 2H), 2.76−2.69 (m, 2H); ^{13}C NMR (CD_3OD) δ 204.2, 172.4, 136.1, 134.2, 129.1 (2 C:s), 128.9 (2 C:s), 128.2 (2 C:s), 127.9, 127.8 (2 C:s), 127.6, 66.2, 59.6, 35.6, 34.4, 27.2. Anal. ($C_{19}H_{21}NO_3$·HCl·0.5 H_2O): C, H, N.

Benzyl (5*S*)-5-Amino-6-methyl-4-oxo-heptanoate (2). Compound **13** (74 mg, 0.20 mmol) was deprotected as described above for **1** to afford 58 mg of **2** (86%) as a white solid: Mp 135−140 °C; $[\alpha]_D$ +8.6° (*c* 1.47, MeOH); ^{1}H NMR (CD_3OD) δ 7.40−7.25 (m, 5H), 5.15 (s, 2H), 4.21 (d, 1H, J = 3.2 Hz), 3.10−3.00 (m, 1H), 2.94−2.68 (m, 3H), 2.62−2.50 (m, 1H), 1.18 (d, 3H, J = 6.8 Hz), 0.96 (d, 3H, J = 7.2 Hz); ^{13}C NMR (CD_3OD)

δ 204.4, 172.4, 136.1, 128.2 (2 C:s), 127.9, 127.8 (2 C:s), 66.1, 63.6, 34.3, 28.4, 27.1, 18.1, 14.9. Anal. ($C_{15}H_{21}NO_3$·HCl): C, H, N.

(2*S*,5*S*)-5-Amino-2-(benzyloxycarbonyl-methyl)-4-oxo-6-phenyl-hexanoic Acid (3). Compound **16** (104 mg, 0.20 mmol) was dissolved in CH_2Cl_2 (2 mL) and TFA (2 mL) and stirred at room temperature for 2 h. The reaction mixture was concentrated under reduced pressure and the residue extracted with water (2 × 10 mL) and diethyl ether (2 × 10 mL). The aqueous phase was concentrated, and the residue was dissolved in the mobile phase and purified with reversed phase preparative HPLC. The combined fractions were evaporated under reduced pressure to give 50 mg of **3** (53%) as a light brownish oil. Also 8 mg (8%) of the (2*R*,5*S*)-epimer was isolated: HPLC, major isomer, t_R 4.3 min; minor isomer, t_R 5.9 min; isomer ratio 90:10.

3: $[\alpha]_D$ +29.7° (*c* 1.12, MeOH); ^{1}H NMR (CD_3OD) δ 7.44−7.30 (m, 10H), 5.15 (app d, 2H), 4.50−4.40 (m, 1H), 3.46−3.36 (m, 2H), 3.17 (dd, 1H, J = 18.4, 7.2 Hz), 2.97 (dd, 1H, J = 14.4, 9.2 Hz), 2.85−2.66 (m, 3H); ^{13}C NMR (CD_3OD) δ 203.5, 175.0, 171.6, 136.0, 134.3, 129.1 (2 C:s), 128.9 (2 C:s), 128.2 (2 C:s), 127.9 (3 C:s), 127.6, 66.2, 59.5, 40.2, 35.9, 35.6, 34.8. Anal. ($C_{21}H_{23}NO_5$·TFA·H_2O): C, H, N.

(2*S*,5*S*)-5-Amino-2-(benzyloxycarbonyl-methyl)-6-methyl-4-oxo-heptanoic Acid (4). Deprotection of **19** (93 mg, 0.20 mmol) as described above for **3** gave 50 mg of **4** (59%) as a light brownish oil. Also 10 mg (12%) of the (2*R*,5*S*)-epimer was isolated: HPLC, major isomer, t_R 2.4 min; minor isomer, t_R 2.9 min; isomer ratio 84:16.

4: $[\alpha]_D$ +43.2° (*c* 1.14, MeOH); ^{1}H NMR (CD_3OD) δ 7.41−7.33 (m, 5H), 5.17 (app d, 2H), 4.16−4.10 (m, 1H), 3.40−3.35 (m, 1H), 3.21 (dd, 1H, J = 18.8, 8.4 Hz), 2.86−2.68 (m, 3H), 2.58−2.48 (m, 1H), 1.17 (d, 3H, J = 7.2 Hz), 0.95 (d, 3H, J = 6.8 Hz); ^{13}C NMR (CD_3OD) δ 203.7, 175.0, 171.6, 136.0, 128.2 (2 C:s), 127.95 (2 C:s), 127.92, 66.2, 63.5, 40.4, 35.8, 34.9, 28.4, 18.2, 14.8. Anal. ($C_{17}H_{23}NO_5$·TFA): H, N; C: calcd, 52.41; found, 51.8.

(5*R*/*S*)-5-Amino-6-(benzyloxycarbonyl)-hexanoic Acid (5). Compound **25** (0.18 mmol, 78.7 mg) was dissolved in CH_2Cl_2 (2 mL) and TFA (2 mL) and stirred at room temperature for 2 h. The reaction mixture was concentrated under reduced pressure and the residue extracted with water (2 × 10 mL) and diethyl ether (2 × 10 mL). The aqueous phase was concentrated to afford 69 mg of **5** (97%) as a brownish oil: ^{1}H NMR (CD_3OD) δ 7.45−7.35 (m, 5H), 5.24 (s, 2H), 4.50 (dd, 1H, J = 7.2, 4.4 Hz), 3.30 (dd, 1H, J = 18.0, 4.0 Hz), 3.10 (dd, 1H, J = 18.2, 7.4 Hz), 2.94−2.76 (m, 2H), 2.67 (app t, 2H); ^{13}C NMR (CD_3OD) δ 202.9, 174.4, 169.5, 135.4, 128.3 (2 C:s), 128.24 (2 C:s), 128.18, 67.2, 55.2, 33.2, 33.0, 27.2. Anal. ($C_{14}H_{17}NO_5$·0.5 TFA·H_2O): C, H, N.

Stability Studies. A. Chemical Stability. The buffers used for stability experiments were HBSS supplemented with 0.05% BSA and 10 mM MES (pH 6.0) (MES-buffer) and 10 mM HEPES (pH 7.4) (HEPES-buffer). The reaction was initiated by adding 100 μL stock solution to 10 mL preequilibrated buffer solution to a final concentration of approximately 10^{-4}−10^{-5} M, and the degradation was studied for several $t_{1/2}$ or over a 48-h period for slower degradations. During the experiments, the solutions were kept in a water bath at 37 °C and at various times, samples were collected and chromatographed immediately. The rates of degradation were determined using HPLC procedures capable of separating BnOH from the model prodrugs.

B. Biological Stability. 10 μL samples were taken from the apical solution at the start and end (t = 0 and 120 min, respectively) of the transport experiments in Caco-2 cell culture (see below). The samples were transferred to HPLC vials and frozen for further analysis by HPLC−UV.

HPLC−UV Quantification. General. For the stability, transport and uptake studies quantification was based on high-performance liquid chromatography (HPLC) and UV-detection (HPLC−UV). A Waters Spherisorb S5OdS2 reversed-phase analytical column (5 μm, 250 × 4.6 mm), a flow rate of 1 mL/min, and UV-detection at 210 nm were used for all HPLC−UV analyses. All quantifications were based on standard curves measured in the concentration range of 10−125 μM. All standard curves yielded regression coefficients (r^2) better than 0.99. The detection and quantification limits (DL and QL, respectively) for **1**−**5** and BnOH on the L-7450 diode array detector were calculated from the standard curves using: QL: 10×(intercept/slope) and DL: 3.3×(intercept/slope). The DL values were 1.9, 7.4, 3.7, 8.5, 10.2, and 1.3 μM for **1**−**5** and BnOH, respectively, and the QL values were 5.8, 22.3, 11.2, 25.9, 30.9, and 0.4 μM for **1**−**5** and BnOH, respectively.

Chemical Stability Studies. HPLC−UV was performed with a system consisting of a Waters pump Model 510, a Waters variable-wavelength UV detector Lambda-Max model 481 spectrophotometer, and a Merck D-2000 GPC integrator. For mobile phase systems and retention times, see Supporting Information.

Biological Stability, Transport and Uptake Studies. HPLC−UV was performed with a Merck/Hitachi system consisting of an L-6000 pump and an L-7450 diode array detector. For mobile phase systems and retention times, see Supporting Information.

Cell Assays. A. Materials. General. Caco-2 cells were obtained from the American Type Culture Collection (Manassas, VA). All chemicals for buffer preparations were of laboratory grade, obtained from Life Technologies and Sigma. Transwell plates (12-well) were from Corning Costar Corporation.

Affinity Studies. [^{14}C]-Gly-Sar (specific activity: 49.94 mCi/mmol) and [^{3}H]-mannitol (specific activity: 51.50 mCi/mmol) were obtained from New England Nuclear. Transepithelial electrical resistance (TEER) was measured in tissue resistance measurement chambers (Endohm) with a voltohmmeter (EVOM), both from World Precision Instruments. The shaking plate used for cell culture experiments was a KS 10 DIGI shaker from Edmund Bühler. Radioactivity was determined in a Packard TriCarb liquid scintillation counter, using Ultima Gold scintillation fluid from Packcard.

Transport and Uptake Studies. Gly-Pro was obtained from Sigma, and [^{3}H]-mannitol from Amersham. The centrifuge was a 1−15K from Sigma, and the sonicator was a Branson sonifier cell disruptor B15.

B. Cell Culture. Caco-2 cells were cultured as previously described.[42] Briefly, cells were seeded in culture flasks and passaged in Dulbecco's Modified Eagle's medium (DMEM) supplemented with 10% fetal bovine serum, penicillin/streptomycin (100 U/mL and 100 μg/mL, respectively), 1% L-glutamine, and 1% nonessential amino acids. Caco-2 cells were seeded onto tissue culture treated 12-well Transwell plates (1.0 cm^2, 0.4 μm pore size) at a density of 10^5 cells × cm^{-2}. Monolayers were grown in an atmosphere of 5% CO_2-95% O_2 at 37 °C. Growth media were replaced every other day. TEER was measured at room temperature before the experiment on day 25−27 post seeding giving TEER = 354 ± 41 Ω × cm^{-2}.

C. Affinity Studies. The affinity experiments were performed as previously described by Nielsen et al.[20] and Våbenø et al.[14] Briefly, the experiment was initiated by adding 0.5 mL of MES-buffer containing 0.5 μCi of [^{14}C]-Gly-Sar and various amounts of the respective compounds to the apical side. Due to the low solubility of **1** in water, **1** was initially dissolved in DMSO and then further diluted in buffer to give the relevant concentration used in the affinity studies. The final DMSO concentration was less than 1.0%, which did not affect the uptake of [^{14}C]-Gly-Sar. A 1.0 mL amount of HEPES buffer was added to the basolateral side of each cell monolayer. During the 5 min incubation, the plates were circularly and continuously shaken. In all experiments the investigated compounds were only applied on the apical side. The temperature was maintained at 37 °C. The uptake of 0.5 μCi [^{14}C]-Gly-Sar was terminated by gentle suction of the uptake medium followed by three washes of the monolayer with ice-cold HBSS. Following the washing step the cells were cut from the Transwell support, placed into scintillation vials and 2 mL of scintillation fluid was added. The cell-associated radioactiv-

ity was counted via liquid scintillation spectrometry. For these experiments, the Hill-factor n was in the range of 0.83−1.31, and U_{max} was between 0.89 and 0.99.

D. Transepithelial Transport across Caco-2 Cell Monolayers. Transport of **1**−**5** and [^{14}C]-Gly-Sar at an apical concentration of 1 mM was measured using MES-buffer as apical media and HEPES-buffer as basolateral media. Similarly, the transport of [^{3}H]-mannitol was measured at an apical concentration of 1 μCi/mL (1.96×10^{-5} M), and BnOH was measured at apical concentrations of 100, 250, and 500 μM. For **1**, the initial stock solution was made in DMSO, and this was then diluted to 1 mM giving a final DMSO concentration of 0.5%. The cell monolayers were rinsed once in prewarmed HBSS. The cells were then incubated for 15 min with MES- and HEPES-buffer on the apical and basolateral sides, respectively, on a shaking plate maintained at 37 °C. After this incubation, the buffers were replaced with the above-mentioned concentrations of the compounds in MES-buffer on the apical side and fresh HEPES-buffer on the basolateral side. 10 μL samples were taken from the apical solution at $t = 0$ and 120 min, and 120 μL samples were taken at 20 min intervals from the basolateral solution and replaced with fresh buffer (t = 40, 60, 80, 100, and 120 min; for BnOH: t = 20, 40, 60, 80, and 100 min). Transport was also measured in the presence of 20 mM Gly-Pro in the apical solution (except for BnOH), in the same manner as described above. Samples were transferred to HPLC vials and frozen for further analysis by HPLC−UV. Samples containing radioisotopes were treated as described in section C, Affinity Studies.

E. Intracellular Uptake in Caco-2 Cell Monolayers. After completion of the 120 min transport study, the cells were rinsed in cold HBSS and detached from the Transwell support using 60 μL of 0.1% Triton X in PBS. Afterward the cell suspension was frozen. Then it was thawed and 120 μL of MilliQ water added, and the cell preparation was lysed using a Branson cell disruptor. The cell suspension was centrifuged for 15 min at 14 000 rpm, and the clear supernatant was used for HPLC−UV analysis.

Data Analysis. 1. Transport Kinetics. A. Affinity. Affinity for hPEPT1 in Caco-2 cells was determined as inhibition of [^{14}C]-Gly-Sar uptake in the presence of varying concentrations of the respective compound. The degree of inhibition was fitted to a Michaelis−Menten type equation:

$$1 - (U/U_0) = \frac{(1 - (U/U_0))_{max} \times [I]^n}{IC_{50}{}^n + [I]^n} \quad (1)$$

where U = uptake of [^{14}C]-Gly-Sar, U_0 = uptake of [^{14}C]-Gly-Sar at zero inhibitor concentration, IC_{50} = the concentration required to inhibit the maximum uptake by 50% (μM), [I] = compound concentration (μM), and n = Hill-factor. K_i values were calculated as described by Cheng and Prusoff[43] using a K_m value for Gly-Sar of 1.1 mM, obtained in our laboratory.

B. Transepithelial Transport. The flux values (J) of the compounds were calculated by:

$$J = \frac{\Delta Q/\Delta t}{A} \quad (2)$$

where $\Delta Q/\Delta t$ is the linear appearance rate of mass in the receiver solution, and A is the cross-section area (1 cm^2). P_{app} values were calculated as $P_{app} = J/C_0$ for mannitol and using non steady-state calculations for BnOH.

C. Uptake. The uptake was calculated as:

$$\text{uptake} = \frac{Q}{A} \quad (3)$$

where Q is the amount of compound (nmol) retrieved in the cell lysate after 2 h and A is the cross-section area (1 cm^2).

2. Stability. The model prodrug degradation rate is proportional to the model prodrug degradation rate constant k and the residual concentration of model prodrug at a given time, t:

$$-\frac{\text{d[model prodrug]}}{\text{d}t} = k[\text{model prodrug}]_t \quad (4)$$

k_{obs} was calculated from first-order degradation kinetics. k_{obs} values were calculated from the linear part of the curve showing $\ln A_{t=0}$ (A = area) as a function of time. The half-life was calculated as $t_{1/2} = \ln 2/k_{obs}$.

3. Statistics Analysis. Unless stated otherwise, values are given as means ± SE, and the statistical significance of the results was determined using two-tailed Student's t-test using GraphPad InStat v3.05. $p < 0.05$ was considered significant. Affinity, transport, and uptake experiments were performed in duplicates (N = 2), in three individual cell passages (n = 3). Stability studies were done in triplicates (n = 3).

Acknowledgment. Financial support for this project was obtained from the Norwegian Research Council (128256/420), the Swedish Research Council (621-2001-1431), the Knut and Alice Wallenberg Foundation (98.176), and the Danish Medicinal Research Council via the Center for Drug Design and Transport and via project grant #22-01-0310. We thank Morten Moe and Trude Anderssen for excellent assistance with MS-MS and analytical and preparative HPLC, and Susanne N. Sørensen, Birgitte Eltong, and Bettina Dinitzen for doing the cell culturing.

Appendix

Abbreviations: Boc: *tert*-butoxycarbonyl; Caco-2: human colonic adenocarcinoma cell line; CoMFA: comparative molecular field analysis; CoMSIA: comparative molecular similarity index analysis; hPEPT1: human di-/tripeptide transporter 1; P_{app}: apparent permeability coefficient (distance × time^{-1}); rPEPT2: rat di-/tripeptide transporter 2; Xaa: any amino acid.

Supporting Information Available: Mobile phase systems and retention times for HPLC analyses in the stability, transport, and uptake studies; elemental analysis data for compounds **1**−**5**. This material is available free of charge via the Internet at http://pubs.acs.org.

References

(1) Fei, Y. J.; Kanai, Y.; Nussberger, S.; Ganapathy, V.; Leibach, F. H.; Romero, M. F.; Singh, S. K.; Boron, W. F.; Hediger, M. A. Expression cloning of a mammalian proton-coupled oligopeptide transporter. *Nature* **1994**, *368*, 563−566.

(2) Liang, R.; Fei, Y. J.; Prasad, P. D.; Ramamoorthy, S.; Han, H.; Yang-Feng, T. L.; Hediger, M. A.; Ganapathy, V.; Leibach, F. H. Human intestinal H$^+$/peptide cotransporter. Cloning, functional expression, and chromosomal localization. *J. Biol. Chem.* **1995**, *270*, 6456−6463.

(3) For representative reviews, see: Walter, E.; Kissel, T.; Amidon, G. L. The intestinal peptide carrier: A potential transport system for small peptide derived drugs. *Adv. Drug Deliv. Rev.* **1996**, *20*, 33−58. Yang, C. Y.; Dantzig, A. H.; Pidgeon, C. Intestinal peptide transport systems and oral drug availability. *Pharm. Res.* **1999**, *16*, 1331−1343. Brodin, B.; Nielsen, C. U.; Steffansen, B.; Frøkjær, S. Transport of peptidomimetic drugs by the intestinal di/tri-peptide transporter, PepT1. *Pharmacol. Toxicol.* **2002**, *90*, 285−296; Rubio-Aliaga, I.; Daniel, H. Mammalian peptide transporters as targets for drug delivery. *Trends Pharmacol. Sci.* **2002**, *23*, 434−440; Nielsen, C. U.; Brodin, B.; Jørgensen, F. S.; Frokjaer, S.; Steffansen, B. Human peptide transporters: therapeutic applications. *Expert Opin. Ther. Pat.* **2002**, *12*, 1329−1350.

(4) Bretschneider, B.; Brandsch, M.; Neubert, R. Intestinal transport of β-lactam antibiotics: Analysis of the affinity at the H$^+$/peptide symporter (PEPT1), the uptake into Caco-2 cell monolayers and the transepithelial flux. *Pharm. Res.* **1999**, *16*, 55−61.

(5) Moore, V. A.; Irwin, W. J.; Timmins, P.; Lambert, P. A.; Chong, S.; Dando, S. A.; Morrison, R. A. A rapid screening system to determine drug affinities for the intestinal dipeptide transporter. 2: Affinities of ACE inhibitors. *Int. J. Pharm.* **2000**, *210*, 29−44.
(6) de Vrueh, R. L. A.; Smith, P. L.; Lee, C. P. Transport of L-valine-acyclovir via the oligopeptide transporter in the human intestinal cell line, Caco-2. *J. Pharmacol. Exp. Ther.* **1998**, *286*, 1166−1170.
(7) Anand, B. S.; Patel, J.; Mitra, A. K. Interactions of the dipeptide ester prodrugs of acyclovir with the intestinal oligopeptide transporter: Competitive inhibition of glycylsarcosine transport in human intestinal cell line-Caco-2. *J. Pharmacol. Exp. Ther.* **2003**, *304*, 781−791.
(8) Taub, M. E.; Moss, B. A.; Steffansen, B.; Frokjaer, S. Influence of oligopeptide transporter binding affinity upon uptake and transport of D-Asp(OBzl)-Ala and Asp(OBzl)-Sar in filter-grown Caco-2 monolayers. *Int. J. Pharm.* **1997**, *156*, 219−228.
(9) Taub, M. E.; Moss, B. A.; Steffansen, B.; Frokjaer, S. Oligopeptide transporter mediated uptake and transport of D-Asp(OBzl)-Ala, D-Glu(OBzl)-Ala, and D-Ser(Bzl)-Ala in filter-grown Caco-2 monolayers. *Int. J. Pharm.* **1998**, *174*, 223−232.
(10) Ezra, A.; Hoffman, A.; Breuer, E.; Alferiev, I. S.; Mönkkönen, J.; El Hanany-Rozen, N.; Weiss, G.; Stepensky, D.; Gati, I.; Cohen, H.; Törmälehto, S.; Amidon, G. L.; Golomb, G. A peptide prodrug approach for improving bisphosphonate oral absorption. *J. Med. Chem.* **2000**, *43*, 3641−3652.
(11) Thomsen, A. E.; Friedrichsen, G. M.; Sørensen, A. H.; Andersen, R.; Nielsen, C. U.; Brodin, B.; Begtrup, M.; Frokjaer, S.; Steffansen, B. Prodrugs of purine and pyrimidine analogues for the intestinal di/tri-peptide transporter PepT1: Affinity for hPepT1 in Caco-2 cells, drug release in aqueous media and in vitro metabolism. *J. Controlled Release* **2003**, *86*, 279−292.
(12) Daniel, H.; Morse, E.; Adibi, S. The high and low affinity transport systems for dipeptides in kidney brush border membrane respond differently to alterations in pH gradient and membrane potential. *J. Biol. Chem.* **1991**, *266*, 19917−19924.
(13) Nielsen, C. U.; Brodin, B.; Jørgensen, F. S.; Frokjaer, S.; Steffansen, B. Human peptide transporters: Therapeutic applications. *Expert Opin. Ther. Pat.* **2002**, *12*, 1329−1350.
(14) Våbenø, J.; Lejon, T.; Nielsen, C. U.; Steffansen, B.; Chen, W.; Ouyang, H.; Borchardt, R. T.; Luthman, K. Phe-Gly dipeptidomimetics designed for the di-/tripeptide transporters PEPT1 and PEPT2: Synthesis and biological investigations. *J. Med. Chem.* **2004**, *47*, 1060−1069.
(15) Taub, M. E.; Larsen, B. D.; Steffansen, B.; Frokjaer, S. β-Carboxylic acid esterified D-Asp-Ala retains a high affinity for the oligopeptide transporter in Caco-2 monolayers. *Int. J. Pharm.* **1997**, *146*, 205−212.
(16) Steffansen, B.; Lepist, E. I.; Taub, M. E.; Larsen, B. D.; Frokjaer, S.; Lennernäs, H. Stability, metabolism and transport of D-Asp-(OBzl)-Ala − a model prodrug with affinity for the oligopeptide transporter. *Eur. J. Pharm. Sci.* **1999**, *8*, 67−73.
(17) Lepist, E. I.; Kusk, T.; Larsen, D. H.; Andersen, D.; Frokjaer, S.; Taub, M. E.; Veski, P.; Lennernäs, H.; Friedrichsen, G.; Steffansen, B. Stability and in vitro metabolism of dipeptide model prodrugs with affinity for the oligopeptide transporter. *Eur. J. Pharm. Sci.* **2000**, *11*, 43−50.
(18) Friedrichsen, G. M.; Nielsen, C. U.; Steffansen, B.; Begtrup, M. Model prodrugs designed for the intestinal peptide transporter. A synthetic approach for coupling of hydroxy-containing compounds to dipeptides. *Eur. J. Pharm. Sci.* **2001**, *14*, 13−19.
(19) Nielsen, C. U.; Andersen, R.; Brodin, B.; Frokjaer, S.; Steffansen, B. Model prodrugs for the intestinal oligopeptide transporter: Model drug release in aqueous solution and in various biological media. *J. Controlled Release* **2001**, *73*, 21−30.
(20) Nielsen, C. U.; Andersen, R.; Brodin, B.; Frokjaer, S.; Taub, M. E.; Steffansen, B. Dipeptide model prodrugs for the intestinal oligopeptide transporter. Affinity for and transport via hPepT1 in the human intestinal Caco-2 cell line. *J. Controlled Release* **2001**, *76*, 129−138.
(21) Thomsen, A. E. Dissertation: *Prodrugs for the di/tripeptide transporter, PEPT1*; The Danish University of Pharmaceutical Sciences: Copenhagen, 2003.
(22) This has been demonstrated for a number of BnOH model prodrugs; see refs 17 and 19.
(23) Sugawara, M.; Huang, W.; Fei, Y. L.; Leibach, F. H.; Ganapathy, V.; Ganapathy, M. E. Transport of valganciclovir, a ganciclovir prodrug, via peptide transporters PEPT1 and PEPT2. *J. Pharm. Sci.* **2000**, *89*, 781−789.
(24) Han, H. K.; de Vrueh, R. L. A.; Rhie, J. K.; Covitz, K. M. Y.; Smith, P. L.; Lee, C. P.; Oh, D. M.; Sadée, W.; Amidon, G. L. 5′-Amino acid esters of antiviral nucleosides, acyclovir, and AZT are absorbed by the intestinal PEPT1 peptide transporter. *Pharm. Res.* **1998**, *15*, 1154−1159.
(25) Deziel, R.; Plante, R.; Caron, V.; Grenier, L.; LlinasBrunet, M.; Duceppe, J. S.; Malenfant, E.; Moss, N. Practical and diastereoselective synthesis of ketomethylene dipeptide isosteres of the type AAΨ[COCH$_2$]Asp. *J. Org. Chem.* **1996**, *61*, 2901−2903.
(26) Våbenø, J.; Brisander, M.; Lejon, T.; Luthman, K. Diastereoselective reduction of a chiral *N*-Boc-protected δ-amino-α,β-unsaturated γ-keto ester Phe-Gly dipeptidomimetic. *J. Org. Chem.* **2002**, *67*, 9186−9191.
(27) Baldwin, J. E.; Adlington, R. M.; Jones, R. H.; Schofield, C. J.; Zaracostas, C.; Greengrass, C. W. γ-Lactam analogues of carbapenicillanic acids. *Tetrahedron* **1986**, *42*, 4879−4888.
(28) Reduction of **8** with H$_2$/Pd−C in EtOAc gave the saturated acid.
(29) Corey, E. J.; Schmidt, G. Useful procedures for the oxidation of alcohols involving pyridinium dichromate in aprotic media. *Tetrahedron Lett.* **1979**, *20*, 399−402.
(30) Wang, S.-S.; Gisin, B. F.; Winter, D. P.; Makofske, R.; Kulesha, I. D.; Tzougraki, C.; Meienhofer, J. Facile synthesis of amino acid and peptide esters under mild conditions via cesium salts. *J. Org. Chem.* **1977**, *42*, 1286−1290.
(31) Significant esterase activity in Caco-2 cell experiments has been reported in other studies: Pauletti, G. M.; Gangwar, S.; Wang, B.; Borchardt, R. T. Esterase-sensitive cyclic prodrugs of peptides: evaluation of a phenylpropionic acid promoiety in a model hexapeptide. *Pharm. Res.* **1997**, *14*, 11−17. Pauletti, G. M.; Gangwar, S.; Okumu, F. W.; Siahaan, T. J.; Stella, V. J.; Borchardt, R. T. Esterase-sensitive cyclic prodrugs of peptides: evaluation of an acyloxyalkoxy promoiety in a model hexapeptide. *Pharm. Res.* **1996**, *13*, 1615−1623. Camenisch, G. P.; Wang, W.; Wang, B.; Borchardt, R. T. A comparison of the bioconversion rates and the Caco-2 cell permeation characteristics of coumarin-based cyclic prodrugs and methylester-based linear prodrugs of RGD peptidomimetics. *Pharm. Res.* **1998**, *15*, 1174−1181.
(32) Covitz, K.-M. Y.; Amidon, G. L.; Sadée, W. Membrane topology of the human dipeptide transporter, hPEPT1, determined by epitope insertions. *Biochemistry* **1998**, *37*, 15214−15221.
(33) Fei, Y. J.; Liu, W.; Prasad, P. D.; Kekuda, R.; Oblak, T. G.; Ganapathy, V.; Leibach, F. H. Identification of the histidyl residue obligatory for the catalytic activity of the human H$^+$/peptide cotransporters PEPT1 and PEPT2. *Biochemistry* **1997**, *36*, 452−460.
(34) Bolger, M. B.; Haworth, I. S.; Yeung, A. K.; Ann, D.; von Grafenstein, H.; Hamm-Alvarez, S.; Okamoto, C. T.; Kim, K. J.; Basu, S. K.; Wu, S.; Lee, V. H. L. Structure, function, and molecular modeling approaches to the study of the intestinal dipeptide transporter PepT1. *J. Pharm. Sci.* **1998**, *87*, 1286−1291.
(35) Yeung, A. K.; Basu, S. K.; Wu, S. K.; Chu, C.; Okamoto, C. T.; Hamm-Alvarez, S. F.; von Grafenstein, H.; Shen, W. C.; Kim, K. J.; Bolger, M. B.; Haworth, I. S.; Ann, D. K.; Lee, V. H. L. Molecular identification of a role for tyrosine 167 in the function of the human intestinal proton-coupled dipeptide transporter (hPepT1). *Biochem. Biophys. Res. Commun.* **1998**, *250*, 103−107.
(36) Kulkarni, A. A.; Haworth, I. S.; Lee, V. H. L. Transmembrane segment 5 of the dipeptide transporter hPepT1 forms a part of the substrate translocation pathway. *Biochem. Biophys. Res. Commun.* **2003**, *306*, 177−185.
(37) Kulkarni, A. A.; Haworth, I. S.; Uchiyama, T.; Lee, V. H. L. Analysis of transmembrane segment 7 of the dipeptide transporter hPepT1 by cysteine-scanning mutagenesis. *J. Biol. Chem.* **2003**, *278*, 51833−51840.
(38) Bailey, P. D.; Boyd, C. A. R.; Bronk, J. R.; Collier, I. D.; Meredith, D.; Morgan, K. M.; Temple, C. S. How to make drugs orally active: A substrate template for peptide transporter PepT1. *Angew. Chem., Int. Ed. Engl.* **2000**, *39*, 506−508.
(39) Gebauer, S.; Knütter, I.; Hartrodt, B.; Brandsch, M.; Neubert, K.; Thondorf, I. Three-dimensional quantitative structure−activity relationship analyses of peptide substrates of the mammalian H$^+$/peptide cotransporter PEPT1. *J. Med. Chem.* **2003**, *46*, 5725−5734.
(40) Weitz, I. S.; Pellegrini, M.; Mierke, D. F.; Chorev, M. Synthesis of a trisubstituted 1,4-diazepin-3-one-based dipeptidomimetic as a novel molecular scaffold. *J. Org. Chem.* **1997**, *62*, 2527−2534.
(41) Müller, P.; Bolea, C. Carbenoid pathways in copper-catalyzed intramolecular cyclopropanations of phenyliodonium ylides. *Helv. Chim. Acta* **2001**, *84*, 1093−1111.
(42) Nielsen, C. U.; Amstrup, J.; Steffansen, B.; Frokjaer, S.; Brodin, B. Epidermal growth factor inhibits glycylsarcosine transport and hPepT1 expression in a human intestinal cell line. *Am. J. Physiol. Gastroint. Liver Physiol.* **2001**, *281*, G191−G199.
(43) Cheng, Y. C.; Prusoff, W. H. Relationship between the inhibition constant (K_I) and the concentration of inhibitor which causes 50% inhibition (I_{50}) of an enzymatic reaction. *Biochem. Pharmacol.* **1973**, *22*, 3099−3108.

JM040780C